

# Many-body interaction in semiconductors probed with 2D Fourier spectroscopy

Mikhail Erementchouk and Michael N. Leuenberger\*  
*NanoScience Technology Center and Department of Physics,  
University of Central Florida, Orlando, FL 32826*

L. J. Sham

*Department of Physics, University of California San Diego, La Jolla, CA 92093-0319*

A particular difficulty in studying many-body interactions in a solid is the absence of an experimental technique that can directly probe their key characteristics. We show that 2D Fourier spectroscopy provides an efficient tool for the measurement of critical parameters describing the effect of many-body interactions on the optical response of semiconductors. We develop the basic microscopic theory of 2D Fourier spectroscopy of semiconductors in the framework of the three-band model (heavy holes, light holes, and electrons). The theory includes many-body correlations nonperturbatively and can be generalized straightforwardly in order to describe 2D Fourier spectra obtained in atomic physics. We establish a relation between the 2D Fourier spectrum and the many-body correlations. It is shown, in particular, that 2D Fourier spectroscopy provides a principal possibility to establish experimentally the origin of the fast decay of the memory term describing the Coulomb interaction between heavy- and light-hole excitons. The theory is applied to an analysis of the available experimental data. Experiments providing more detailed information are suggested.

Understanding many-body interactions in solids is one of the key problems of modern solid state physics (see, for instance, the recent review Ref. 1). The long-range Coulomb interaction between electrons leads to complex dynamics of the excitations in semiconductors and plays the principal role in the nonlinear optical response. Different experimental techniques have been developed for studying the effects of many-body interactions. One of the most popular experiments is based on the four-wave mixing (FWM)<sup>2</sup>. In these experiments the sample is illuminated by rays characterized by (non-parallel) wave vectors  $\mathbf{k}_1$ ,  $\mathbf{k}_2$ , and  $\mathbf{k}_3$ . The outgoing signal is detected in the direction that corresponds to the nonlinear coupling of the excitation pulses, say,  $-\mathbf{k}_1 + \mathbf{k}_2 + \mathbf{k}_3$ . The advantage of such measurements is that the many-body contribution to the signal is not blurred by the strong linear (single-particle) component. The sensitivity of the FWM spectrum to the details of the interaction between the excitons and other many-body excitations makes it an efficient tool for probing the many-body properties. However, the standard FWM experiment does not allow one to make a distinction between different contributions of many-body interactions and correlations to the shape of the resonance. As a result it is difficult to interpret a FWM spectrum and to extract specific characteristics of the many-body interactions and correlations.

Recently the more flexible technique of two-dimensional Fourier spectroscopy<sup>3,4,5</sup> has been applied to studying the semiconductor properties<sup>6,7</sup>. The general scheme is similar to that of standard time-resolved FWM experiments with three pulses propagating along  $\mathbf{k}_1$ ,  $\mathbf{k}_2$ , and  $\mathbf{k}_3$  launched at  $t = t_1$ ,  $t_2$ , and  $t_3$ , respectively. The difference from a standard FWM experiment is that measurements are performed not at a fixed or just a few values of the delay time  $\tau = \min(t_2, t_3) - t_1$ , but rather for a dense series of values lying in some interval. Subsequently, the Fourier transforms are done with

respect to the delay time as well as with respect to the signal time. These two Fourier transforms constitute the two-dimensional Fourier spectrum. It is important to emphasize that in the experiments reported in Refs. 6,7 the difficult problem of measuring both the real and the imaginary parts of the signal was resolved. These experiments, therefore, provide the information about the phase acquired during the delay time. As will be shown below, this allows one to make a distinction between the diffraction on the gratings created by the heavy- and the light-hole excitons. Thus, 2D Fourier spectroscopy experiments give substantial insight into the details of the many-body correlations and provide vital information, which is barely accessible using the standard approach. Despite many advantages provided by the 2D Fourier spectroscopy, the application of this technique suffers from the lack of the understanding of the spectra from the microscopic standpoint. Usually, 2D Fourier spectra are described in the framework of the phenomenology of the nonlinear susceptibility, which hides the relation between features of the spectra and the microscopic characteristics of the system.

Here we develop the basic microscopic theory of 2D Fourier spectroscopy of the semiconductors in the framework of the three-band model (heavy holes, light holes, and electrons). We use the perturbational approach with respect to the excitation field. The interaction between the excitons, on the contrary, is taken into account exactly. We show that the 2D Fourier spectrum gives the unique opportunity to measure the key quantities describing the exciton-exciton interaction. We use our theory to analyze the experimental results of Ref. 6. Our calculations produce relations between the spectral features of the 2D Fourier spectrum and the parameters characterizing the many-body interaction that allow us to suggest experiments that would provide more detailed information. Because of the generality of the approach,

our theory is able to describe also the 2D Fourier spectra of other physical systems, such as molecular nanostructures.

The basic idea behind the derivation of the equations of motion of the exciton polarization is that the states with the definite number of particles are the eigenstates of the Hamiltonian of the unperturbed (i.e. without external field) semiconductor. Initially, before the first pulse hits the sample, the system is assumed to be in the vacuum state  $|0\rangle$  with full valence and empty conduction bands. The excitation pulses couple the eigenstates of the system populating, thereby, states with different number of particles. The excitation pulses create directly  $P_\kappa^{(l)}$ , the linear response polarization. This excitation is described in the rotating-wave approximation by

$$\left(\frac{\partial}{\partial t} + i\omega_\kappa + \Gamma_\kappa\right) P_\kappa^{(l)} = -dE_{\sigma_\kappa}^{(l)}(t), \quad (1)$$

where  $l = 1, 2, 3$  enumerates the exciton pulses according to their time order. Here and below the Greek letters

$\kappa, \lambda, \mu, \nu$  are multi-indices denoting the exciton state according to  $\kappa = \{n_\kappa, \sigma_\kappa\}$ , where  $n_\kappa$  is the type of the exciton equal to h or to l for heavy-hole and light-hole excitons, respectively, and  $\sigma_\kappa$  is the helicity of the state. In Eq. (1) we have introduced  $\Gamma_\kappa$  as the decay rate of the exciton state  $\kappa$ , and  $\omega_\kappa$  as the detuning, which is the difference between the frequency of the rotating frame and the exciton frequency  $\tilde{\omega}_\kappa$ . The external source is specified by the dipole moment  $d$  and by the component of the  $l$ -th pulse,  $E_{\sigma_\kappa}^{(l)}(t)$ , with the helicity  $\sigma_\kappa$ . The linear responses  $P_\kappa^{(l)}$ , in turn, serve as sources of the third-order polarization. The dynamics of the third-order polarization is conveniently written in terms of the operator  $D_{\mu\nu} = [B_\mu, [B_\nu, H]]$ , where  $H$  is the Hamiltonian of the unperturbed semiconductor and the operator  $B_\mu^\dagger$  creates an exciton in the state  $\mu$ . The dynamics of the polarization corresponding to the FWM signal in the direction  $-\mathbf{k}_l + \mathbf{k}_m + \mathbf{k}_n$ , where  $l, m$ , and  $n$  enumerate the excitation pulses, is governed by<sup>8</sup>

$$\begin{aligned} \left(\frac{\partial}{\partial t} + i\omega_\kappa + \Gamma_\kappa\right) P_\kappa = \sum_{\lambda, \mu, \nu} \left\{ -i\beta_{\mu\nu}^{\kappa\lambda} P_\lambda^{(l)*} P_\mu^{(m)} P_\nu^{(n)} + \frac{1}{2} P_\lambda^{(l)*} \int_{t_0}^t dt' e^{-(\Gamma_\mu + \Gamma_\nu)(t-t')} F_{\mu\nu}^{\kappa\lambda}(t-t') P_\mu^{(m)}(t') P_\nu^{(n)}(t') \right. \\ \left. - id C_{\mu\nu}^{\kappa\lambda} P_\lambda^{(l)*} \left[ P_\mu^{(m)} E_{\sigma_\nu}^{(n)}(t) + P_\mu^{(n)} E_{\sigma_\nu}^{(m)}(t) \right] \right\}. \end{aligned} \quad (2)$$

The parameters  $\beta$  and the memory functions  $F$  describe the effect of the exciton-exciton correlations. Obviously, interactions involving higher number of particles do not contribute to the third-order polarization. These parameters are defined by  $\beta_{\mu\nu}^{\kappa\lambda} = \langle D_{\kappa\lambda} B_\mu^\dagger B_\nu^\dagger \rangle$  and  $F_{\mu\nu}^{\kappa\lambda}(\tau) = \langle e^{iH\tau} D_{\kappa\lambda} e^{-iH\tau} D_{\mu\nu}^\dagger \rangle$ . The last term in Eq. (2) accounts for the Pauli blocking with the phase-space filling parameters<sup>8</sup>  $C_{\mu\nu}^{\kappa\lambda}$ .

As follows from Eqs. (1) and (2) we need to take into account only the excitons with helicity of unit magnitude, i.e. the ones coupled to the one-photon states of electromagnetic field. Therefore, in what follows, we will consider only excitons with  $\sigma_\kappa = \pm 1$ .

We would like to emphasize that Eq. (2) exactly accounts for the Coulomb interaction between excitons. The generality of the basic ideas and non-restrictive assumptions make this equation virtually model-independent. However, in order to present the relation between the 2D Fourier spectrum and the parameters characterizing the many-body interaction in the most transparent way, we restrict ourselves to the short-memory approximation.<sup>8</sup> The effect of non-locality of the memory function on the 2D Fourier spectrum will be investigated elsewhere. The short-memory approximation corresponds to relatively short biexciton life time<sup>8</sup> or fast decay of the memory function.<sup>9,10</sup> In the framework of

this approximation the last term in the r.h.s. of Eq. (2) is substituted by an instantaneous term, which we absorb into the modified  $\beta$ -parameter defining

$$\tilde{\beta}_{\mu\nu}^{\kappa\lambda} = \beta_{\mu\nu}^{\kappa\lambda} + \gamma_{\mu\nu}^{\kappa\lambda}. \quad (3)$$

In what follows we will refer to  $\tilde{\beta}$  as the modified mean-field parameter, outlining that it is local in time.

The exact form of  $\gamma_{\mu\nu}^{\kappa\lambda}$  depends on the origin of the fast decay of the kernel. In the simplest case of short life-time one has<sup>8</sup>

$$\gamma_{\mu\nu}^{\kappa\lambda} = \frac{i}{2(\Gamma_\mu + \Gamma_\nu)} F_{\mu\nu}^{\kappa\lambda}(0). \quad (4)$$

In the case of the fast decay of the memory function<sup>9,10</sup> the modification of the  $\beta$ -parameter takes the form

$$\gamma_{\mu\nu}^{\kappa\lambda} = \frac{1}{2} \left\langle D_{\kappa\lambda} \frac{1}{H - i(\Gamma_\mu + \Gamma_\nu)} D_{\mu\nu}^\dagger \right\rangle. \quad (5)$$

We study the polarization mixing induced by the many-body interaction using the standard three band (electrons, heavy, and light holes) semiconductor model, where the exciton destruction operator has the form  $B_\mu = \int dx dy B_\mu(x, y)$  with

$$B_\mu(x, y) = \phi_\mu^*(x - y) v_{\sigma_\mu(1)}^\dagger(y) c_{\sigma_\mu(2)}(x). \quad (6)$$

Here  $\phi_\mu(x-y)$  is the exciton envelope wave function,  $v$  and  $c$  are the annihilation operators acting on the states in the valence band and the conduction band, respectively. The indices  $\sigma_\kappa(i)$  specify the spin of the electron in the valence ( $i=1$ ) and conduction ( $i=2$ ) bands. In terms of  $B_\mu(x,y)$  one can explicitly write<sup>11</sup>

$$D_{\mu\nu} = \int dx_1 \dots dy_2 B_\mu(x_1, y_1) B_\nu(x_2, y_2) U(x_1, y_1; x_2, y_2), \quad (7)$$

where  $U$  is the energy of the electrostatic interaction between two excitons.

From the definitions of  $\tilde{\beta}_{\mu\nu}^{\kappa\lambda}$  and  $\gamma_{\mu\nu}^{\kappa\lambda}$  one can derive the spin selection rules. It can be shown that the contribution of the  $\beta$ -term reduces to  $\propto -i\beta_{\bar{\kappa}}^{\kappa} |P_{\bar{\kappa}}|^2 P_{\kappa} - i\beta_{\bar{\kappa}}^{\bar{\kappa}} |P_{\bar{\kappa}}|^2 P_{\bar{\kappa}}$ , where  $\bar{\kappa}$  denotes the exciton state ‘‘conjugate’’ to  $\kappa$ , with the conjugation understood according to the rule  $\{h, \pm 1\} \leftrightarrow \{1, \mp 1\}$ . The  $\gamma$ -term turns out to be less restrictive having the form  $\propto \sum_{\lambda} \gamma_{\kappa}^{\lambda} |P_{\lambda}|^2 P_{\kappa}$ .

For both  $\beta$  and  $\gamma$  the reduction of the indices is performed according to the same rule  $\tilde{\beta}_{\kappa}^{\lambda} = \tilde{\beta}_{\bar{\kappa}}^{\kappa\lambda} (2 - \delta_{\kappa\lambda})$ . The expressions for  $\beta$  and  $\gamma$  are combined together to the modified mean-field term according to Eq. (3). In what follows we treat  $\tilde{\beta}_{\kappa}^{\lambda}$  as phenomenological parameters. It suffices for our purposes since we are interested in a relation between the 2D Fourier spectral features and the microscopic characteristics rather than in first-principle calculations of 2D Fourier spectra.

We consider the 2D Fourier spectrum obtained in the so-called rephasing scheme<sup>12</sup>, when the excitation pulse corresponding to the conjugated field arrives first, i.e.  $l=1$  in Eqs. (1) and (2). Resolving these equations with respect to the FWM polarization  $P_{\kappa}$  and performing the Fourier transform with respect to both the signal time  $t$  and the delay time  $\tau = \min(t_2, t_3) - t_1$ , we obtain for  $P_{\kappa}(\omega, \Omega)$  the expression

$$P_{\kappa} = d|d|^2 \sum_{\lambda} \tilde{\beta}_{\kappa}^{\lambda} \frac{E_{\sigma_{\lambda}}^{(1)*} \left[ E_{\sigma_{\lambda}}^{(2)} E_{\sigma_{\kappa}}^{(3)} e^{-2\Gamma_{\lambda}T} + E_{\sigma_{\lambda}}^{(3)} E_{\sigma_{\kappa}}^{(2)} f_{\kappa}^{\lambda}(T) \right] g_{\lambda}(\tau_{\max})}{(\omega - \omega_{\kappa} + i\Gamma_{\kappa})(\omega - \omega_{\kappa} + i\Gamma_{\kappa} + 2i\Gamma_{\lambda})(\Omega + \omega_{\lambda} + i\Gamma_{\lambda})} + \Pi_{\kappa}(\omega, \Omega), \quad (8)$$

where  $\Pi_{\kappa}(\omega, \Omega)$  is the Pauli blocking contribution to the 2D spectrum

$$\Pi_{\kappa}(\omega, \Omega) = -|d|^2 d \sum_{\lambda, \mu, \nu} C_{\mu, \nu}^{\kappa, \lambda} \frac{E_{\sigma_{\lambda}}^{(1)*} E_{\sigma_{\mu}}^{(3)} E_{\sigma_{\nu}}^{(2)} f_{\nu}^{\lambda}(T) g_{\lambda}(\tau_{\max})}{(\omega - \omega_{\kappa} + i\Gamma_{\kappa})(\Omega + \omega_{\lambda} + i\Gamma_{\lambda})}. \quad (9)$$

In Equations (8) and (9) the function  $f_{\kappa}^{\lambda}(T) = e^{-T[i(\omega_{\kappa} - \omega_{\lambda}) + \Gamma_{\kappa} + \Gamma_{\lambda}]}$  describes the dependence of the spectrum on the time separation of the second and the third pulses  $T = t_3 - t_2$ , the frequencies  $\omega$  and  $\Omega$  correspond to the signal time and the delay time, respectively, and  $E_{\sigma}^{(m)} = \int dt E_{\sigma}^{(m)}(t)$ . Deriving Eqs. (8) and (9) we have used the assumption that the pulses are short compared to the characteristic dynamical time scales determined by  $\omega_{\kappa}$  and  $\Gamma_{\kappa}$ . The function  $g_{\lambda}(\tau_{\max}) = 1 - e^{i\tau_{\max}(\Omega + \omega_{\lambda} + i\Gamma_{\lambda})}$ , with  $\tau_{\max}$  being the maximal reached value of the delay time, accounts for the finite range of the delay time used in the experiments and explains the wavy character of the spectrum along the vertical axis.

As follows from Eqs. (8) and (9) the spectrum has resonances in the 2D  $(\omega, \Omega)$ -plane at points with the coordinates  $(\omega_{\mu}, -\omega_{\nu})$ . It is seen that a particular exciton state  $\kappa$  produces only one resonance along the  $\omega$ -axis. The resonances along the  $\Omega$ -axis are produced by the nonlinear coupling of the exciton state  $\kappa$  with different exciton states. Such a separation between the interaction with heavy- and light-hole excitons is possible solely due to the structure of the 2D Fourier spectrum.

Simple comparison of Eqs. (9) and (8) shows that the

2D spectra of the FWM signal created by the Pauli blocking and the Coulomb interaction between the excitons have qualitatively different form. The resonances on the spectrum produced by the Pauli blocking have the Lorentz form along the vertical and horizontal axes. The reason is that the dependence of the signal on the signal and delay time is essentially the free evolution of the polarization created by a short pulse. This evolution has the form of oscillations, which produce a simple pole after the Fourier transform. At the same time the resonances created by the Coulomb interaction fall off asymptotically as  $\propto 1/\Omega$  and as  $\propto 1/\omega^2$ , along the  $\Omega$ - and  $\omega$ -axes, respectively. This is the direct consequence of the fact that the FWM polarization is continuously excited by the polarizations of the linear response. The dependence on the signal time is found as a convolution of the respective Green function with the source. After the Fourier transform with respect to signal time it yields the product of Fourier images of the Green function and the source. This results in the asymptotic form  $\propto 1/\omega^2$  because of the harmonic time dependence of these functions.

More detailed consideration of the spectrum depends on the specific experimental situation. Keeping in mind the analysis of the experiments reported in Refs. 6,7, we make several simplifying assumptions. First of all we note that the experimental spectra corresponding to the rephasing scheme have clear elongation along the vertical axis. According to the discussion above this means that the main contribution to the FWM spectrum in these

experiments comes from the Coulomb interaction. We employ this observation by neglecting the Pauli blocking term  $\Pi_\kappa(\omega, \Omega)$  in Eq. (8). Additionally, we assume that the helicities of the excitation pulses and the detected signal are not resolved. Thus, the signal is obtained as a sum of contributions (8). Also, we assume that the basic exciton characteristics do not depend on helicity, so that we have only two sets of parameters corresponding to light-hole and heavy-hole excitons. As a result, one ends up with four resonances in the  $(\omega, \Omega)$ -plane, situated near the vertices of a square. Finally, we take  $T = 0$ .

$$\mathcal{E}_\mu^\nu(\omega, \Omega) = i \frac{A_\mu^\nu}{(\omega - \omega_\mu + i\Gamma_\mu)(\omega - \omega_\mu + i\Gamma_\mu + 2i\Gamma_\nu)(\Omega + \omega_\nu + i\Gamma_\nu)}, \quad (10)$$

where

$$A_\mu^\nu = \frac{2\pi l}{nc} \bar{\omega}_{n_\mu} d |d|^2 \sum_{\sigma_\mu, \sigma_\nu} \tilde{\beta}_{n_\mu, \sigma_\mu}^{n_\nu, \sigma_\nu} E_{\sigma_\nu}^{(1)*} \left( E_{\sigma_\nu}^{(2)} E_{\sigma_\mu}^{(3)} + E_{\sigma_\nu}^{(3)} E_{\sigma_\mu}^{(2)} \right). \quad (11)$$

We note that as follows from this expression  $A_\mu^\nu = A_{n_\mu}^{n_\nu}$ , i.e. these parameters depend only on the type of the excitons because of the summation over helicities. However, in order to improve readability of formulas, we keep the general notations where it is necessary. In Eq. (11)  $l$  is the thickness of the sample,  $n$  is the refractive index of the material, and  $c$  is the speed of light. The magnitude of  $\mathcal{E}_\mu^\nu(\omega, \Omega)$  has the simplest form. It is a product of pole functions. The real and imaginary parts of the signal demonstrate a more complex structure. For example, the real part of the resonance,  $R_\mu^\nu$ , near the point  $(\omega_\mu, -\omega_\nu)$  changes its sign along the curve  $R_\mu^\nu(\omega, \Omega) = 0$ , which in a vicinity of  $(\omega_\mu, -\omega_\nu)$  can be approximated by a straight line

$$R_\mu^\nu(\omega, \Omega) = \arg(A_\mu^\nu) + \frac{2(\Gamma_\mu + \Gamma_\nu)}{\Gamma_\mu(\Gamma_\mu + 2\Gamma_\nu)}(\omega - \omega_\mu) + \frac{1}{\Gamma_\nu}(\Omega + \omega_\nu). \quad (12)$$

We apply the developed description of the 2D Fourier spectrum for the analysis of the experimental data obtained in Refs. 6. We would like to start from noting that, as follows from Eq. (12), the slope of the zero line  $R_\mu^\nu(\omega, \Omega) = 0$  is the constant  $-4/3 \approx -1.33$ . The experimental value of the slope is found to be equal to  $-1.3$ . We would like to stress the universality of the slope and to emphasize that such a good agreement with the experiment is provided by the fact that the  $(\omega_h, -\omega_h)$ -resonance is the strongest one and the slope of the zero line is weakly affected by other resonances. The slope, however, strongly depends on the dynamical model describing the exciton polarization. In particular, if one takes into account the Pauli blocking then the slope would take value depending on the relation between the Coulomb interac-

tion and the Pauli blocking contributions into the FWM spectrum. The slope takes the value  $-4/3$  in the limit when the Pauli blocking can be neglected.

From the experimental data of Ref. 6 we find the parameters  $A_\mu^\nu$  using the least-square method. The exciton parameters  $\omega_\mu$  and  $\Gamma_\mu$  are tuned in order to minimize the deviation between the theory and the experiment. The results of the fit are shown in Table I. The 2D Fourier spectrum corresponding to the fitted parameters is depicted in Fig. 1.

The difficulty of extracting more detailed information from the results of Ref. 6 is that the measurements were

TABLE I: Fitted values of the parameters of the system studied in Ref. 6. The values of the exciton frequencies are provided in the stationary frame.

$n$	$\omega_n$ , meV	$\Gamma_n$ , meV	$A_n^h$	$A_n^l$
h	1540	1.3	$8.1 - i4.6$	$6.0 + i9.3$
l	1544	1.7	$0.7 - i9.9$	$12.3 + i1.5$

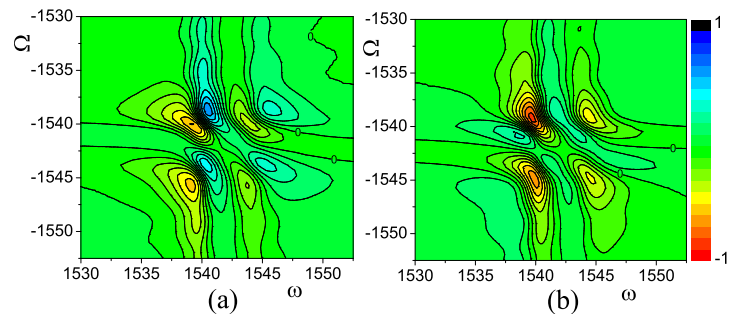


FIG. 1: The real part (a) and the imaginary part (b) of the 2D Fourier spectrum obtained using the parameters from Table I. These figures should be compared with Figs. 7e and 7f of Ref. 6.

tion and the Pauli blocking contributions into the FWM spectrum. The slope takes the value  $-4/3$  in the limit when the Pauli blocking can be neglected.

From the experimental data of Ref. 6 we find the parameters  $A_\mu^\nu$  using the least-square method. The exciton parameters  $\omega_\mu$  and  $\Gamma_\mu$  are tuned in order to minimize the deviation between the theory and the experiment. The results of the fit are shown in Table I. The 2D Fourier spectrum corresponding to the fitted parameters is depicted in Fig. 1.

The difficulty of extracting more detailed information from the results of Ref. 6 is that the measurements were

performed using linearly polarized pulses and the linearly polarized signal was detected. Much more detailed information can be obtained if the signals with circular polarization, i.e. with fixed helicity, are used. As follows from Eq. (11) a particular choice of the helicities of the excitation pulses and the detected signal allows a direct access to particular  $\tilde{\beta}$ 's. For example, if the excitation pulses have helicity  $\sigma = +1$  and a signal with  $\sigma = +1$  is detected, then each resonance in  $(\omega, \Omega)$ -plane will be determined by the specific  $\tilde{\beta}_{n_{\mu},+1}^{n_{\nu},+1}$ . It is interesting to note that this provides the principal possibility to obtain experimentally the information about the origin of the fast decay of the memory term describing the Coulomb interaction between the heavy- and light-hole excitons. Indeed, this particular choice of the helicities excludes the contribution from the interaction between  $\{h, +1\}$  and  $\{l, -1\}$  excitons, so that only the term  $\propto \gamma_{h,+1}^{l,+1}$  will mostly contribute. If the memory decay is caused by the short biexciton life-time then, as follows from Eq. (4), this should result in imaginary  $\tilde{\beta}_{1,+1}^{h,+1}$ . This will not be the case if the respective matrix elements of  $F_{\mu\nu}^{\kappa\lambda}(t)$  decay faster<sup>9</sup> than  $1/(\Gamma_{\mu} + \Gamma_{\nu})$ .

We would like to note that even more flexible access to different matrix elements of  $\tilde{\beta}_{\mu}^{\nu}$  is provided by the observational scheme with the time separating second and third pulses equal to the delay time,  $T = \tau$ . In this scheme the different sequences of excitation pulses, which enter symmetrically Eq. (8), turn out to produce different resonances along  $\Omega$ -axis. As a result, the 2D Fourier spectrum obtained using this scheme has four resonances along the vertical axis separated by  $\omega_l - \omega_h$ .

We conclude by considering briefly the effect of inhomogeneous broadening. The broadening is taken into account by averaging the spectrum with respect to a joint distribution of the exciton frequencies. First, we note the different effect of the inhomogeneous broadening on the diagonal and off-diagonal resonances. While averaging is performed the resonances situated near  $(\omega_{\mu}, -\omega_{\mu})$  move along the diagonal resulting in elongating resonances in this direction. At the same time the width

of the resonance in the direction perpendicular to the diagonal does not change and is determined by the homogeneous linewidth. As follows from Eq. (10), the half-width in the perpendicular direction  $\delta_{\mu}$  of the magnitude of the signal near  $(\omega_{\mu}, -\omega_{\mu})$  is found from the equation  $(\delta_{\mu}^2 + 2\Gamma_{\mu}^2)^2(\delta_{\mu}^2 + 18\Gamma_{\mu}^2) = 144\Gamma_{\mu}^6$  and is equal to  $\delta_{\mu} \approx 0.88\Gamma_{\mu}$ . Applying this relation to the spectra obtained in Ref. 6 we obtain  $\Gamma_h \approx 1.2\text{meV}$  and  $\Gamma_l \approx 1.4\text{meV}$ , which are in a agreement with the values found in Table I.

The effect of the inhomogeneous broadening on the off-diagonal resonances is determined by the relation between the distributions of the frequencies of the heavy-hole and light-hole excitons. For not too high values of the broadening the value of the light-hole – heavy-hole splitting can be considered to be fixed. As a result, averaging leads to elongation of the off-diagonal resonance along respective line, whose slope depends on the ratio between the values of inhomogeneous broadenings of the light-hole and heavy-hole excitons.

In summary, we have developed the basic microscopic theory of 2D Fourier spectroscopy of semiconductors. We have shown that the resonant peculiarities in 2D Fourier spectrum are directly related to respective microscopic quantities describing the exciton-exciton interaction. Because of the two-dimensional structure of the spectrum the contributions from the Coulomb interaction between different excitons (heavy- and light-hole) turn out to be naturally separated. We demonstrate, in that way, that 2D Fourier spectroscopy provides a unique opportunity to extract the information regarding many-body correlations in semiconductors from direct measurements. In particular, we show that it is possible to obtain experimentally the information regarding the origin of the fast decay of the memory term describing the Coulomb interaction between the heavy-hole and light-hole excitons. We have given a simple application of the theory analyzing the experimental data reported in Ref. 6.

We would like to thank Xiaoqin Li and Steve Cundiff for useful discussions. This work is supported by NSF DMR 0403465.

\* Electronic address: mleuenbe@mail.ucf.edu

<sup>1</sup> D. Chemla and J. Shah, *Nature* **411**, 549 (2001).

<sup>2</sup> S. Mukamel, *Principles of nonlinear optical spectroscopy* (Oxford University Press, New York, 1995).

<sup>3</sup> M. Khalil, N. Demirdoven, and A. Tokmakoff, *J. Phys. Chem. A* **107**, 5258 (2003).

<sup>4</sup> D. M. Jonas, *Annual Rev. Phys. Chem.* **54**, 425 (2003).

<sup>5</sup> V. Cervetto, J. Helbing, J. Breidenbeck, and P. Hamm, *J. Chem. Phys.* **121**, 5935 (2004).

<sup>6</sup> T. Zhang, C. Borca, X. Li, and S. Cundiff, *Opt. Express* **13**, 7432 (2005).

<sup>7</sup> X. Li, T. Zhang, C. Borca, and S. Cundiff, *Phys. Rev. Lett.*

**96**, 057406 (2006).

<sup>8</sup> T. Ostreich, K. Schonhammer, and L. J. Sham, *Phys. Rev. B* **58**, 12920 (1998).

<sup>9</sup> S. Savasta, O. Di Stefano, and R. Girlanda, *Phys. Rev. Lett.* **90**, 096403 (2003).

<sup>10</sup> S. Savasta, O. Di Stefano, and R. Girlanda, *Semicond. Sci. Technol.* **18**, S294 (2003).

<sup>11</sup> L. J. Sham and T. Ostreich, *J. Luminescence* **87-89**, 179 (2000).

<sup>12</sup> R. Boyd, *Nonlinear Optics* (Academic Press, San Diego, 2002).